

Ultra low-loss low-efficiency diffraction gratings

T. Clausnitzer, E.-B. Kley, A. Tünnermann

Institut für Angewandte Physik, Friedrich-Schiller Universität, Max-Wien Platz 1, 07743 Jena, Germany
clausnitzer@iap.uni-jena.de

A. Bunkowski, O. Burmeister, K. Danzmann, R. Schnabel

Max-Planck-Institut für Gravitationsphysik and Institut für Atom- und Molekülphysik, Universität Hannover,
Callinstrasse 38, 30167 Hannover, Germany

S. Gliech, A. Duparré

Fraunhofer-Institut für Angewandte Optik und Feinmechanik, Albert-Einstein-Str. 7, 07745 Jena, Germany

Abstract: The realization of ultra low-loss dielectric reflection gratings with diffraction efficiencies between 7% and 0.02% is presented. By placing the grating beneath the highly reflective layerstack scattering was significantly reduced. This concept allows the all-reflective coupling of high laser radiation to high finesse cavities, thereby circumventing thermal effects caused by absorption in the substrate.

©2005 Optical Society of America

OCIS codes: (050.1950) Diffraction gratings, (120.3180) Interferometry, (230.1360) Beam splitters

References and links

1. T. Clausnitzer, J. Limpert, K. Zöllner, H. Zellmer, H.-J. Fuchs, E.-B. Kley, A. Tünnermann, M. Jupé, and D. Ristau, „Highly efficient transmission gratings in fused silica for CPA systems,” *App. Opt.* **42**, 6934-6938 (2003)
2. Z. S. Liu, S. Tibuleac, D. Shin, P.P. Young, R. Magnusson, “High-efficiency guided mode resonance filter,” *Opt. Lett.* **23**, 1556-1558 (1998)
3. T. Clausnitzer, A.V. Tishchenko, E.B. Kley, J. Fuchs, D. Schelle, O. Parriaux, U. Kroll, “Narrow band, polarization independent free space wave notch filter,” accepted for publication in *JOSA A*
4. T. Clausnitzer, H.-J. Fuchs, E.-B. Kley, A. Tünnermann, U. D. Zeitner, „Polarizing metal stripe gratings for a micro-optical polarimeter,” in *Lithographic and Micromachining Techniques for Optical Component Fabrication II*, E.B. Kley, H. P. Herzig, eds., *Proc. SPIE* **5183**, 8-15 (2003)
5. B. Willke et.al., “The GEO 600 gravitational wave detector,” *Class. Quantum Grav.* **19**, 1377-1387 (2002)
6. R. W. P. Drever, “Concepts for Extending the Ultimate Sensitivity of Interferometric Gravitational Wave Detectors Using Non-Transmissive Optics with Diffractive or Holographic Coupling,” in *Proceedings of Seventh Marcel Grossman Meeting on General Relativity*, M. Kaiser and R. T. Jantzen, eds., 1401-1406 (1995)
7. A. Bunkowski, O. Burmeister, P. Beyersdorf, K. Danzmann, R. Schnabel, T. Clausnitzer, E.-B. Kley, A. Tünnermann, “Low-loss grating for coupling to a high-finesse cavity,” *Opt. Lett.* **29**, 2342-2344 (2004)
8. A. Bunkowski, O. Burmeister, K. Danzmann, and R. Schnabel, “Input-output relations for a three-port grating coupled Fabry-Perot cavity,” *Opt. Lett.* **30**, 1183-1185 (2005)
9. B. W. Shore, M. D. Perry, J. A. Britten, R. D. Boyd, M. D. Feit, H. T. Nguyen, R. Chow, G. E. Loomis, and Lifeng Li, “Design of high-efficiency dielectric reflection gratings,” *J. Opt. Soc. Am. A* **14**, 1124-1136 (1997)
10. M. D. Perry, R. D. Boyd, J. A. Britten, D. Decker, B. W. Shore, C. Shannon, E. Shults, “High-efficiency multilayer dielectric reflection gratings,” *Opt. Lett.* **20**, 940-942 (1997)
11. K. Hehl, J. Bischoff, U. Mohaupt, M. Palme, B. Schnabel, L. Wenke, R. Bödefeld, W. Theobald, E. Welsch, R. Sauerbrey, and H. Heyer, “High-Efficiency Dielectric Reflection Gratings: Design, Fabrication, and Analysis,” *Appl. Opt.*, **38**, 6257-6271 (1999)
12. J. Turunen, “Diffraction theory of microrelief gratings,” in *Micro-optics*, H.P. Herzig, ed. (Taylor & Francis, Inc., 1997)
13. A. Duparré, J. Ferre-Borrull, S. Gliech, G. Notni, J. Steinert, J. M. Bennett, „Surface characterization techniques for determining the root-mean-square roughness and power spectral densities of optical components,” *Appl. Opt.* **41**, 154-171 (2002)

14. E.-B. Kley, T. Clausnitzer, M. Cumme, K. Zöllner, B. Schnabel, A. Stich, "Investigation of Large-Area Gratings Fabricated by Ultrafast E-Beam Writing," in *Advanced Optical Manufacturing and Testing Technology*, L. Yang, H. M. Pollicove, Q. Xin, J. C. Wyant, eds., Proc. SPIE **4231**, 116-125 (2000)
15. J. Stover, *Optical Scattering – Measurement and Analysis*, (SPIE, Bellingham, WA, 1995)
16. A. Duparré, "Light scattering of thin dielectric films," in *Handbook of Optical Properties - Thin Films for Optical Coatings*, R.E. Hummel, K.H. Guenther, eds. (CRC Press, Boca Raton, 1995)
17. L. Li, J. Hirsh, "All-dielectric high-efficiency reflection gratings made with multilayer thin-film coatings," *Opt. Lett.* **20**, 1349-1351 (1995)
18. J. K. Guha, J. A. Plascyk, "Low-Absorption Grating Beam Samplers," in *Optical Components: Manufacture and Evaluation*, D. Nicholson ed., Proc. SPIE **171**, 117-124 (1979)

1. Introduction

During recent years the progress of microlithographic fabrication techniques has opened up a large number of new exciting applications for grating structures, as for example in high-power laser systems [1] or as a substitute for conventional optical devices such as narrow band spectral filters [2,3] or polarizers [4]. Due to the high reproducibility of the grating features, good quality gratings for most applications became commercially. However, for some challenging applications where extremely high efficiencies or low losses are required, the employment of gratings is only beginning. One example is gravitational wave detection with Michelson interferometers. The sensitivity of such detectors depends on the circulating laser power as well as the propagation length. Both values can be improved by applying signal and power-recycling mirrors as was done in GEO 600 [5]. The next generation GW interferometers will employ laser sources of 200 W single mode radiation. Techniques like power recycling and Fabry Perot cavities in the arms of the interferometer will provide circulating powers of megawatts. For such high powers residual absorption even in the best substrates available, will lead to thermal effects, which will limit the performance of the system. Thus, new concepts using all-reflective optics for interferometers are currently under investigation. Reference [6] proposes some setups that include reflective gratings as beam splitters or as cavity couplers. The performance of these devices (damage resistance, losses) is a limiting factor for the whole interferometer. In this paper we want to focus on a cavity coupler. This coupler can be realized by high-efficiency gratings in 1st order Littrow mounting [Fig. 1(a)], where the specular low-efficiency 0th order is used to couple light to the cavity, as well as by low-efficiency gratings in 2nd order Littrow-mounting [Fig. 1(b)], where the weak – 1st order, propagating normally to the substrate, is used for the coupling. A higher diffraction efficiency, however, tends to require a heavier treatment of the initial flat surface. It can thus be roughly assumed that the losses of a grating increase with diffraction efficiency, so that the second approach seems to be more beneficial. Recently we have demonstrated the realization of a high finesse cavity using low-efficiency dielectric reflection gratings [7]. The aim of this work is to show how the diffraction efficiency of such gratings can be controlled and the scattering losses reduced.

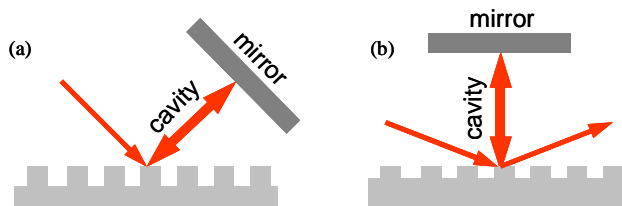


Fig. 1. Gratings as cavity coupler (a) high efficiency grating: coupling by the specular 0th order (b) low efficiency grating: coupling by the weak -1st diffraction order

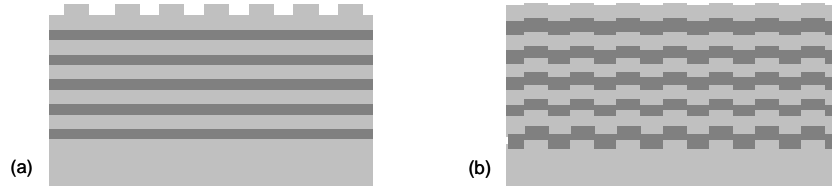


Fig. 2. Two approaches to combine grating and layerstack: (a) grating on top, (b) grating beneath the stack

2. General considerations on the sample design

The dielectric reflective cavity coupler grating consists of a substrate, a dielectric multilayer, and the grating itself. The scattering losses of the whole device are influenced by the quality of all three components. For our investigations we used substrates with a surface deformation of less than $\lambda/10$ as well as a standard coating process for low loss dielectric mirrors. Our investigations will therefore only regard the scattering caused by the grating, the majority of which is due to roughness of the grating grooves as well as periodical or statistical variations of the groove shape. The combination of grating and HR-stack can be done in two different ways. Either the grating can be made in the topmost layer of the stack [Fig. 2(a)], or secondly it can be etched into the substrate followed by coating of the multilayer stack [Fig. 2(b)]. The way in which the grating and layerstack are combined significantly influences the scattering as well as the transmission. Both layouts will be discussed in the next sections. In the cavity setup we used in [7], the gratings are illuminated in 2nd order Littrow mounting. The low-efficiency -1^{st} order is used to couple light to the cavity in a direction normal to the substrate, as shown in Fig. 3(a) (for a theoretical description of the cavity concept see Reference [8]). The finesse of the cavity built by the grating device and a highly-reflective mirror is determined by the reflectivities of both components [Fig. 3(b)]. The reflectivity of the grating in the case of normal incidence (R_{0°) is influenced by losses like transmission through the substrate (T) and scattering (S), as well as by the efficiency of diffraction in the two first orders (η_i). As it was fabricated with binary electron-beam lithography, the grating can be assumed to have rectangular and therefore symmetrical grooves. The two orders therefore have the same efficiency. The marked arrows in Fig. 3 illustrate that the -1^{st} order in Fig. 3(a) propagates through the same optical path as the -1^{st} order in Fig. 3(b), and the diffraction efficiency (η_i) is therefore the same in both cases. This means that when the grating couples light to the cavity with an efficiency of η_i , the 0^{th} -order reflectivity of the grating for normal incidence is given by

$$R_{0^\circ} = 1 - (2\eta_1 + T + S). \quad (1)$$

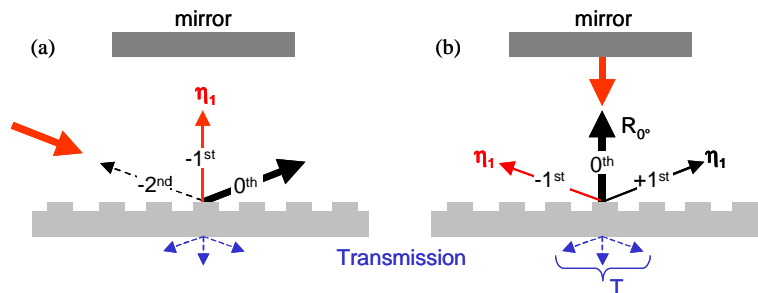


Fig. 3. (a) Incidence from 2nd order Littrow angle and (b) retroreflection for normal incidence. The transmission T (blue) is defined as the sum of all transmitted diffraction orders. Due to the same optical path h_1 is the same in (a) and (b) (red arrows).

Our general goal is a high power build-up in the cavity, which requires reduction of the transmission T as well as the scattering losses S . The finesse of the cavity is determined by the value of R_{ρ} . Hence, for fixed values of S and T , the finesse can be controlled by changing η_l . For the devices discussed above, the aim was to realize efficiencies in the range below 5%.

The propagation directions of the diffraction orders of a grating in air are given by the grating equation

$$\sin \varphi_m = \sin \varphi_{in} + \frac{m\lambda}{d}, \quad (2)$$

where λ is wavelength, d the grating period, φ_{in} the incident angle, and φ_m the propagation angle of the m_{th} diffraction order. The setup demands that the -1^{st} order propagates normally to the grating. That is, for the incident beam

$$\sin \varphi_{in} = \frac{\lambda}{d}. \quad (3)$$

Since φ_{in} has to be smaller than 90° in air, the period has to be larger than the wavelength. A further issue is that every propagating order carries an amount of energy. In order to reduce scattering losses by additional diffraction orders, only those orders that are going to be used in the setup should be allowed to propagate. The period is thus restricted to less than 2λ . The wavelength the devices are designed for is 1064 nm (Nd:YAG- laser). Therefore, periods between 1064 nm and 2128 nm are eligible.

The transmission losses of the device are primarily determined by the layerstack. Figure 4 shows the measured angular reflectivity (s-polarized light) of the stack used here, layered on a plane substrate. The multilayer stack consists of 36 alternating films of Ta_2O_5 (refractive index $n = 2.02$) and SiO_2 ($n = 1.45$). It was designed for a reflectivity higher than 99.95% between 0° and 70° . For the theoretical calculations in the next section, thicknesses of 137 nm and 193 nm have been assumed for the Ta_2O_5 and the SiO_2 layers, respectively.

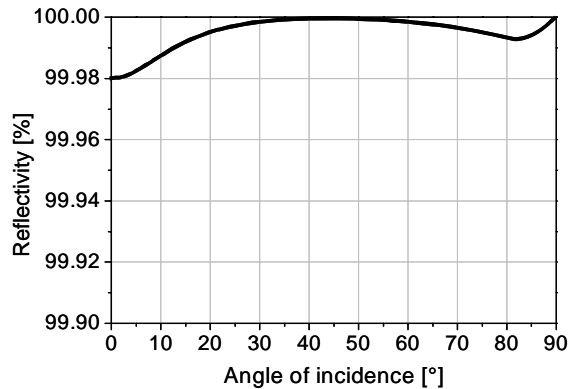


Fig. 4. Measured reflection spectrum of the dielectric layerstack composed of Ta_2O_5 and SiO_2 ($\lambda = 1.064\mu\text{m}$)

3. Grating on top of the HR stack

The practice of putting a grating on top of a highly reflective layerstack is a well-established technique for high-efficiency dielectric reflection gratings [9-11]. The parameters to be optimized are the depth of the grating grooves, which are etched into the topmost layer of the HR-stack, and the thickness of the residual layer beneath the grating. The sum of these two layers results in the required thickness of the topmost layer, which can be either the high or

low refractive index material. We chose fused silica because its etching behaviour is very well investigated. For the grating-etching step it is favourable to choose a thickness t of this last layer such that the diffraction properties change only slowly when the groove depth is changed. To find the proper layer thickness theoretical calculations using the rigorous Fourier Modal Method [12] have been performed. A grating fill factor (ratio between ridge width and period) of 0.5 and TE-polarized illumination was assumed. Figure 5 shows the calculated diffraction efficiency η_1 in the case of a grating period of $1.45\mu\text{m}$, as a function of the groove depth h_g and the thickness t_r of the residual fused silica layer beneath the grating. The 2nd order Littrow angle is 47.1° for this period [Eq. (3)]. The dashed curves in Fig. 5 highlight the area where the efficiency is between 1% and 5%. For a thickness t of 550 nm, an efficiency of about 2.5% can be achieved for groove depths between 150 nm and 350 nm (along the straight line). This large tolerance is very beneficial for the grating-etching step.

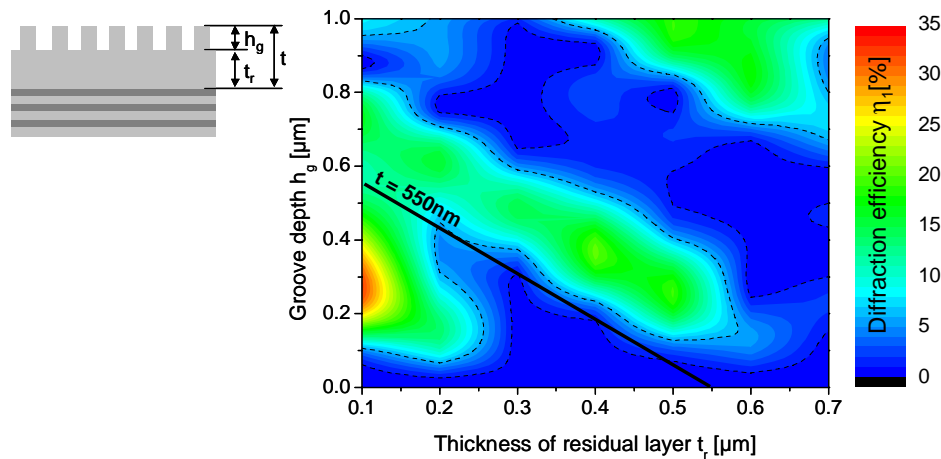


Fig. 5. Theoretical calculation of the diffraction efficiency as a function of groove depth h_g and the thickness of the residual layer beneath the grating t_r .

For fabrication of the HR-stack, a flat fused silica substrate has been coated first by ion beam sputtering. In accordance with Fig. 5 we chose fused silica with a thickness of 550 nm as the topmost layer. The grating with a $1.45\mu\text{m}$ period was fabricated by electron-beam lithography and reactive ion beam etching. A groove depth of 290 nm and a fill factor of 0.5 were measured by an atomic force microscope (AFM). If the grating grooves were ideal, the grating would theoretically possess a diffraction efficiency of $\eta_1 = 1.5\%$ and thus a reflectivity of $R_\phi = 97\%$ [Eq. (1)]. To analyze the losses of the real gratings we measured the angle-resolved scattering (ARS) using the high-sensitivity ARS-instrumentation described in [13]. These measurements, of course, do not provide the value of the total scattering S of the device. Estimation of total scattering by either direct measurement with an integrating or a Coblentz sphere or by calculation from measured ARS curves still rises several problems, which are a topic of further detailed studies. These investigations address the question how to estimate and even how to define the total scattering for a grating - and in particular the value of the angle separating efficiency from scatter - in harmony with the instructions given for plane surfaces in the international standard ISO 13696. However, the ARS-measurements give insight into the scattering processes and are a good measure for S . The samples were illuminated by a Nd:YAG laser at 1064 nm wavelength, TE-polarization, and normal incidence. Figure 6 shows the results of these measurements. A first order diffraction efficiency of 1.5% was also measured by a calibrated integrating sphere. Beside the expected peaks there are some additional diffraction peaks in the range of 10^{-6} of the incident intensity between the 0th and the two first orders. These orders are a result of periodic fill factor

variations that are typical for e-beam lithographic pattern generation [14]. The scattering reveals a largely uniform decay over the whole space surrounding the grating, which is an indication for statistical roughness-induced scattering [15]. These losses might be reduced by low-pass filtering the grating structure. It is well-known that dielectric coatings can smooth a profile [16]. Consequently, covering a grating structure with a dielectric layer is a possible way to remove high frequency perturbations like roughness or sharp edges. If the smoothing is very strong only the period information is retained, therefore statistical or systematical fill factor variations can be removed. This is the idea of the following concept.

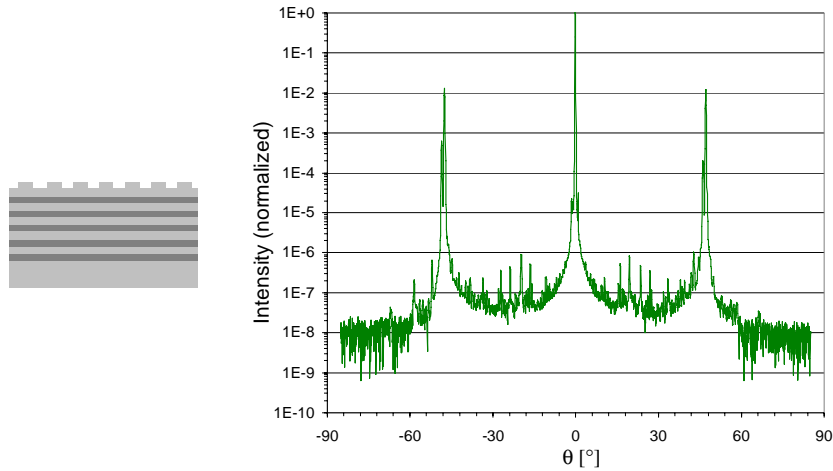


Fig. 6. Angle resolved scattering measurement of the grating on top of the multilayer ($\lambda = 1.064\mu\text{m}$)

4. Grating beneath the HR stack

A smoothing of the grating profile as described in the previous paragraph can be achieved if the grating is first fabricated on a substrate and then coated with the HR-stack. This approach has been experimentally used to realize all-dielectric high efficiency reflection gratings [17] or low absorption low efficiency grating beam samplers [18]. A detailed theoretical analysis of this layout has been done for example by Elson [19]. However, simulation of the diffraction efficiencies of such a device is much more complicated than in the previous approach, because the layer growth on a structured substrate has to be included. We therefore investigated these elements empirically. One important issue to be considered here is the deformation of the layerstack by the grating. When the grating is on top, the layerstack is not disturbed by the grating; its reflectivity can be optimized like a simple laser mirror. Here, the surface relief of the grating influences the layer growth, so it will have a modified –and certainly increased– transmission. On the other hand the number of layers and the resulting profile smoothing form a volume grating with variable corrugation depending on the penetration depth of the light and the shape of the grating beneath. Thus, by changing the profile of the primary grating, the diffraction efficiency of the grating device, its transmission, and its scattering can be influenced or tuned.

To investigate this issue we placed gratings with several fill factors on one substrate and covered them with standard HR-layerstacks as used in the grating-on-top-concept. In Fig. 7 the cross-section of several gratings with a groove depth of 40 nm and 150 nm (measured before the coating process by AFM) is illustrated. The corrugation depth of the volume grating is obviously decreased by increasing the number of layers. Small fill factors and therefore narrow grating ridges disturb the layerstack more than larger fill factors. However, if Fig. 7(a) and Fig. 7(b) are compared, the surface reliefs become nearly equal after a certain number of

layers, independent from the depth of the original grating. It is therefore likely that the coating also smooths roughness and sharp edges.

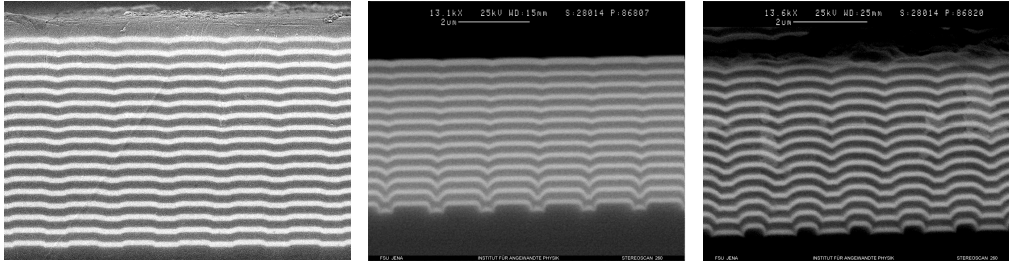


Fig. 7. Scanning electron microscope images of coated gratings
 (a) original groove depth 40 nm, fill factor 0.52
 (b) original groove depth 150 nm, fill factor 0.67
 (c) original groove depth 150 nm, fill factor 0.33

We measured the value of η_l as well as the 0th transmitted order with an integrating sphere. Since the diffraction of the grating is set to be weak, measuring the 0th transmitted order is a good estimation for the whole transmission of the sample. The measurement results are shown in Fig. 8(a) and (b) (black and red lines). The dashed line in Fig. 8(b) indicates the transmission of the substrate without perturbation by the grating. As discussed above, a smaller fill factor causes a larger corrugation of the volume grating, resulting in higher diffraction efficiency and transmission. For larger fill factors the corrugation is smoother, and the diffraction efficiency approaches zero, and the transmission becomes comparable to an undisturbed mirror. Furthermore, the graphs for the 150 nm-deep gratings approach those of the 40 nm-deep gratings if the fill factor increases. This fact confirms the observations already made in the SEM-images. To quantify the scattering losses ARS-measurements were again performed for selected gratings.

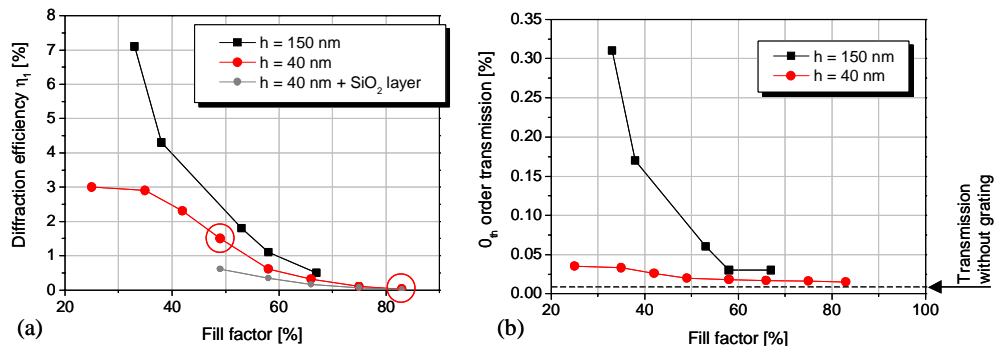


Fig. 8. (a) Diffraction efficiency and (b) 0^o transmission measured by an integrating sphere

Figure 9 shows the measurement results of two gratings with a depth of 40 nm and fill factors of 0.49 and 0.83 (illustrated by the hollow circles in Fig. 8(a)). In Fig. 9(a) the intensity of the two first orders is nearly the same as in Fig. 6. Thus, this grating fills nearly the same optical function. The scattered light, however, is significantly reduced. There is only one parasitic diffraction order with an intensity of 10^{-6} between the 0th and the two first orders; the other peaks are in the range of 10^{-7} or less, while in Fig. 6 all parasitic orders are higher than $5 \cdot 10^{-7}$. Also, the background signal caused by statistical roughness is reduced from $3 \cdot 10^{-8}$ to $1 \cdot 10^{-8}$. In Fig. 9(b) the scattering is further decreased, and only one parasitic order could be

resolved by the measurement setup. Therefore the coating smooths not only the statistical errors but also periodical variations of the fill factor.

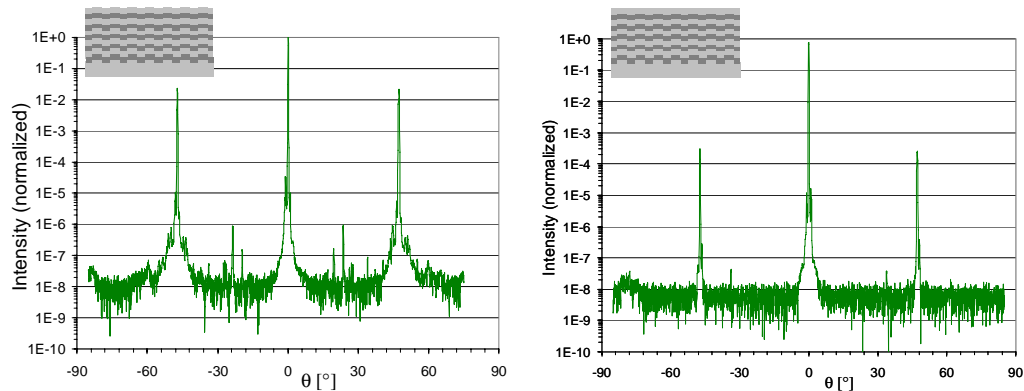


Fig. 9. Angle resolved scattering measurement ($\lambda = 1064$ nm) of gratings coated by the multilayer
(a) fill factor = 0.49 (b) fill factor = 0.67

It can be concluded from these measurements that scattering in diffractive cavity couplers can be efficiently reduced by placing a thick dielectric layerstack on top of the grating. Because of the resultant smoothing the resulting surface profile looks very similar for all the profiles considered here; roughness, sharp edges, and even small periodic fill factor variations are suppressed. The transmission is slightly enhanced compared to the undisturbed mirror. A smaller difference could be achieved by increasing the thickness of the layerstack. The smoothing of the grating profile is strongly influenced by the applied deposition technology and its parameters. A detailed analysis of the SEM-images showed that a layer consisting of SiO_2 changes the corrugation much more than a layer consisting of Ta_2O_5 , which is a result of different angular distributions of the sputter particles during the ion beam coating process used here. Instead of increasing the number of layers we therefore prepared a sample by inserting a $1.5\mu\text{m}$ thick layer of fused silica between the grating and the HR-stack. The measured diffraction efficiencies are illustrated by the grey line in Fig. 8(a), in comparison to the other samples. While for smaller fill factors these are significantly different from the samples without this additional layer, the two graphs approach each other for larger values. Obviously the large fill factor profiles have reached a limiting surface corrugation, which is hardly changed by additional coatings. Figure 10 shows the ARS-measurements for the largest fill factor grating. The first order efficiency is comparable to Fig. 9(b), but the small peaks near 35° are not observable anymore. For this grating a transmission of 10^{-4} was measured, which is the same as for the undisturbed mirror.

5. Conclusions

We have investigated the realization of low-efficiency dielectric reflection gratings by two concepts: gratings made on top of a highly reflective layerstack and the converse assembly. By coating the multilayer on top of the grating the losses of a grating can be effectively reduced. High-frequency profile features such as roughness, sharp edges or periodical fill factor variations are decreased, as are the scattering losses. The smoothing of the surface corrugation also corresponds to a decrease in diffraction efficiency. This effect can be used to tune the diffraction efficiency. Diffraction efficiencies between 7% and 0.02% have been demonstrated, with ultra low scattering losses. For a grating with 1.5% diffraction efficiency, a reduction of the angle-resolved scattering losses from $3 \cdot 10^{-8}$ to $1 \cdot 10^{-8}$ due to statistical scattering has been demonstrated, while parasitic diffraction orders have been drastically reduced.

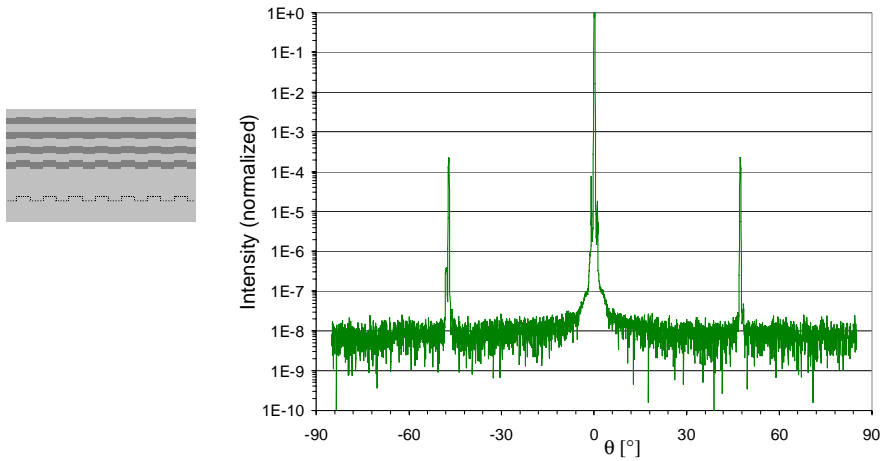


Fig. 10. Angle resolved scattering measurement ($\lambda = 1064$ nm) of a grating coated by a $1.5\mu\text{m}$ thick SiO₂ layer and the HR-stack

Acknowledgments

This work was supported by the German Research Association (DFG) within the Sonderforschungsbereich TR 7 “Gravitational Wave Astronomy”. The authors would like to thank Layertec Optical Coatings GmbH for the coating of the dielectric stacks and Dr. U. Hübner (IPHT Jena) for the high-resolution SEM-images.